Experimental Studies of Ablation Surface Patterns and Resulting Roll Torques

E. P. WILLIAMS*
McDonnell Douglas Astronautics Company—West, Huntington Beach, Calif.

Because of the interest in differential ablation patterns and their implications for the roll characteristics of small hypervelocity vehicles, conical models covered with various low-temperature ablative materials were tested in a hypersonic wind tunnel. A unique feature of these tests was the direct measurement of roll torques during the actual ablation process. These tests were conducted at Mach 6 on sharp-nosed models, mostly subliming camphor and special Korotherm. The scale of cross-hatching is shown to decrease with increasing pressure for camphor. The ablation pattern of melting-vaporizing naphthalene is similar to that of subliming camphor. The cross-hatched pattern of subliming Korotherm in the wind tunnel is found to be similar to that of silica phenolic in flight. Some rolling moment coefficient data are presented.

Nomenclature

A = ablation age $\equiv W/\delta$
C_l = rolling-moment coefficient = rolling moment/qSd
d = model base diameter
M = Mach number
P = pressure
q = dynamic pressure, $\frac{1}{2}\rho V^2$
S = model base area
T = temperature
t = time
W = thickness of material ablated away
α = angle of attack
δ = boundary-layer thickness
θ = cone half angle
λ = ablation surface pattern length (Fig. 8)
ϕ = ablation surface pattern half angle
ω = spin rate

Subscripts

∞ = freestream conditions
e = boundary-layer edge
L = local
o = initial
r = recovery conditions
T = total or stagnation conditions
w = wall conditions

Introduction

INTRIGUING ablation patterns on meteorites and tektites have been noted and studied for decades.[1-4] Chapman and Larson have studied the ablation patterns of tektites and have produced the characteristic ring-wave flow ridges in the laboratory.[2,3] Examples of both streamwise grooves and regmaglypt† ablation on meteorites are shown in the photographs of Ref. 1 and 4.

The recognition of crosshatched ablation patterns is more recent. Tests of the control fin area of a high-performance interceptor in the NASA Huntsville chemical jet facility during 1962 caused the formation of a crosshatched pattern on the Teflon ramp ahead of the fin as shown in Fig. 1. The proximity of the cross-hatching angle to the test stream Mach angle led to speculation that grooves might have resulted from nonuniform flow in the combustion jet. This explanation was invalidated, however, when similar patterns were observed on several vehicles that were recovered from subsequent flight tests. Occasionally, an isolated radial groove was found in the Teflon nose. These radial grooves usually followed a discontinuity in the local surface slope or some other disturbance.

The NASA Ames Research Center has been very active in studying ablation surface patterns, including cross-hatching, and has conducted many ballistic range and hypersonic wind-tunnel experiments.[4-8] Larson and Mateer noted the development of cross-hatching on camphor models into a pattern that resembled the regmaglypt pattern observed on many meteorites.[4] The same phenomenon is confirmed by the wind-tunnel tests reported in this paper. Canning, Wilkins, and Tauber have reported on turbulence wedges, streamwise grooves, and crosshatched patterns from their ballistic range and wind-tunnel tests and proposed a physical flow model to explain these patterns.[5,7,8]

Laganelli and Nestler have reported the results of tests in the Malta rocket exhaust facility and the NASA Langley 8-ft structures tunnel on a wide variety of materials, ranging from wood to carbon phenolic.[9] Particular emphasis was placed on char-forming materials.

At the time the tests reported herein were planned, information available indicated that certain gross features and trends characterized surface ablation pattern phenomena, as follows. 1) The local inviscid flow must be supersonic or hypersonic ($M_e > 1$). 2) A turbulent, or at least transitional, boundary layer is required to form the patterns. 3) The local surface pressure must exceed 600 psf. 4) Appreciable ablation must occur. 5) The pattern cant angle variation with M_e follows the trend of Mach angle, at least for moderately supersonic edge Mach numbers. 6) Cross-hatching occurs on

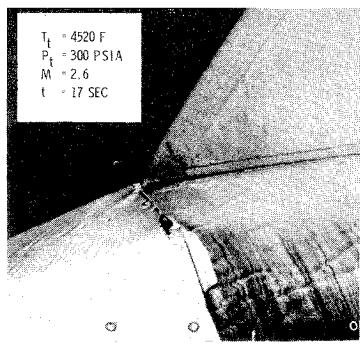

Fig. 1 Cross-hatching of teflon ramp in NASA Huntsville 164-HT-Burner.

Presented as Paper 69-180 at the AIAA 7th Aerospace Sciences Meeting, New York, January 20–22, 1969; submitted February 19, 1969; revision received March 10, 1971.

* Senior Staff Engineer, Advance Missile and Re-Entry Systems. Associate Fellow AIAA.

† From the Greek regma (rhēgma) meaning to break or fracture and glyptic (glyptos) meaning to carve.

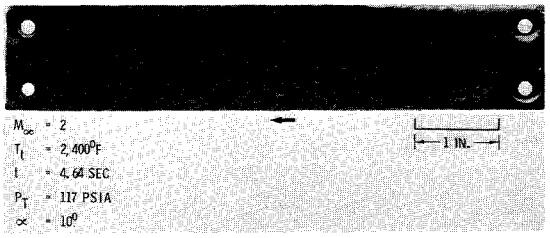

Fig. 2 Korotherm 320 after ablation in MDAC-West Aeroder Facility.

both two-dimensional and axisymmetric bodies. This is not necessarily a complete list of phenomenology recognized at the time of test planning, but includes the major pertinent items. The third item in the list was based on the test results of Ref. 6, which indicated cross-hatching on camphor cones at 840 psf but not at 420 psf; this item was modified as a result of the MDAC-West tests, which produced cross-hatching at a local surface pressure as low as 170 psf. A subsequent exception to the ablation requirement (No. 4) is the Aeronautical Research Associates of Princeton (ARAP) test of grease by jet impingement.

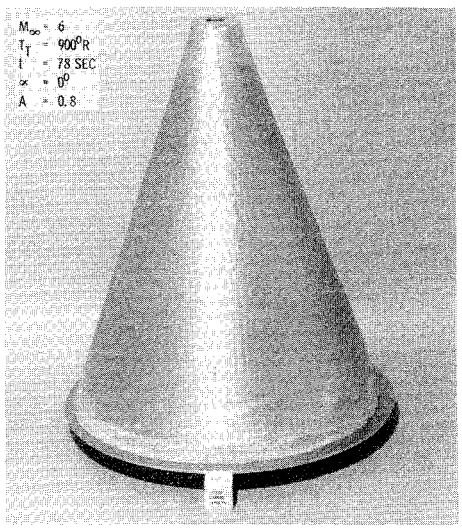

Fig. 3a 20° camphor cone tested at surface pressure of 170 psf.

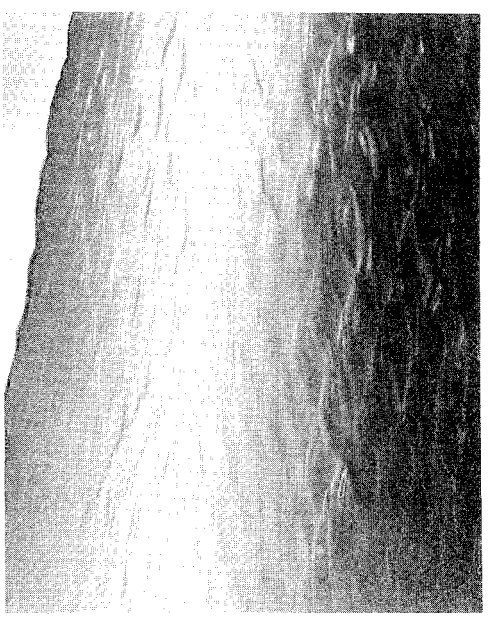

Table 1 Model geometry

Cone half angle, deg	Base diameter, in.	Length, in.
20	13	17.9
25	12	12.9
30	10	8.7
35	9.4	6.7

Apparatus and Models

Wind-Tunnel and Model Selection

The tests were conducted in the Douglas Aerophysics Laboratory 2-ft hypersonic wind tunnel.[10] This facility operates by blowdown from a 3500 psi storage reservior through a pebble-bed furnace to a vacuum of approximately 3 psia supplied by air-driven ejectors. The tunnel is equipped with axisymmetric contoured nozzles for generation of test Mach numbers of 6, 8, and 10. Tests were performed by first establishing preselected, steady-state stream conditions; quickly injecting the model into the stream for the desired test time; and then retracting the model before shutting down the tunnel.

The redundant operating constraints of a hypersonic wind tunnel, coupled with the phenomenology requirements for local turbulent, supersonic flow in the presence of appreciable ablation with a local surface pressure of greater than 600 psf, created an interesting model selection problem. This is discussed in Ref. 11. At Mach 6 the highest pressure and Reynold's number is achieved for this tunnel and consequently the greatest turbulent flow.‡ Therefore, all tests were conducted at a freestream Mach number of 6. The freestream total pressure was varied from 250 to 650 psia and the total temperature was varied between 900° and 1400°R. Right circular cone geometry was selected because of the plans for torque measurements. Pointed steel tips were chosen to ensure known vertex geometry and to avoid boundary-layer transition suppression from nose bluntness. The choice of cone angle and cone length were constrained by tunnel blockage and boundary-layer transition considerations as well as the minimum local surface pressure allowable for crosshatching. The actual model geometry selected is shown in Table 1.

Model Ablative Materials

A variety of low-temperature ablators was tested, as indicated in Table 2. Korotherm 320 is a low-temperature spray-on ablator that is used, for example, on ascent stages. Crosshatched patterns developed on this material in the MDAC-West Aeroder (Fig. 2) suggested its use in the hyper-

Table 2 Wind-tunnel test matrix

Materials	Cone half angle 20°	25°	30°	35°
Camphor	●	●	○ ●	●
Naphthalene			●	
Special korotherm		●	○ ●	●
Lexan			●	
Lucite			●	
Korotherm 320			●	
Local flow conditions			$M_\infty = 6_\infty$	
$2.3 \leq M_L \leq 3.8$			$\alpha = 0°$ ●	
170 psf $\leq P_L \leq$ 1100 psf			$\alpha = 5°$ ○	
900°R $\leq T_T \leq$ 1400°R				

‡ Boundary-layer transition occurred within the first 30% of the model length for all the ablating models except the aft ablation only model (Fig. 12).

sonic wind tunnel. Similar, but less pronounced, patterns were also developed in Insulcork. The Aeroder is a Mach 2 ceramic heated air-jet facility. Because standard, off-the-shelf Korotherm 320 did not ablate sufficiently in the hypersonic wind tunnel at Mach 6, a special lower ablation temperature Korotherm was supplied by the manfactuer (DeSoto, Incorporated, Berkeley, California) for these tests. Korotherm has advantages over camphor because it is relatively stable at room temperature and, in the subliming mode, produces a wind-tunnel crosshatched pattern that is more similar to that of phenolic, fused-silica-fiber in flight. Special Korotherm[§] was either cast or troweled on the model aluminum core; the conical surface was readily machined on a contour lathe.

Camphor and naphthalene models were made by sintering the powered material over an aluminum core in a vacuum under high pressure. The conical surface was then machined on a contour lathe. The vacuum sintering process produces a much stronger and more satisfactory model than previous casting (NASA Ames) or dipping (GASL[12]) techniques. Sayano and Charwat report approximately a 60% increase in the shear strength of vacuum sintered camphor over that of cast and dipped camphor and a much greater increase for naphthalene.[13,14] This process is believed to have been first used by Sayano and Charwat, who pressed small models uniaxially with a piston. Because of the difficulty of pressing large models uniaxially and for ease of attachment of the models to the wind-tunnel balance and sting, MDAC-West developed the technique of isostaticly pressing over an aluminum core. For more fabrication details, see Refs. 11–14.

Some experience was also acquired with naphthalene, which behaves somewhat differently from camphor. Naphthalene remains opaque when pressed in a vacuum either uniaxially or isostaticly. It is more difficult to make satisfactory models of naphthalene. Sayano and Charwat suggest this is possibly because naphthalene is composed of leaflet-shaped particles, which are less suited to compression sintering than the hexagonal crystals of camphor.[13,14] Nevertheless, naphthalene models were successfully fabricated and tested to show the effect of a liquid layer on the ablation pattern. (Camphor sublimed under the test conditions.)

Instrumentation and Data

A very sensitive (3 in.-lb) strain-gage, flexural pivot, almost frictionless, roll-torque balance was used to measure the small roll torque resulting from surface ablation patterns. The accuracy of this balance was quite satisfactory for measuring rolling moment coefficients of the order of 10^{-5}.

Calibration showed balance readings to be repeatable to within 0.25% of the full scale reading (3 in.-lb). Bendix Free-Flex pivots are used in this balance instead of a more conventional roll bearing. These pivots consist of flat, crossed springs that support rotating sleeves. There is no friction between the moving parts, which are entirely interconnected by the flexing springs. Digital rolling moment data were recorded at intervals of from 0.2 to 0.8 sec during each entire run A Sanborn recorder was also used to give an approximate but continuous record of roll torque.

The model was monitored on closed circuit television during the tests. Two 16-mm Milliken motion-picture cameras were mounted above the model and 90° apart. Both cameras were operated at a speed of 64 frames/sec, usually with color film. In addition, either shadowgraphs or Schlieren pictures were taken intermittently during the test. Rubber molds (either RTV-11 or ADRUB) were made of the models shortly after the tests and epoxy casts were made later for a more permanent record of the ablated surface patterns. In addition, pretest and post-test model pictures and measurements were obtained.

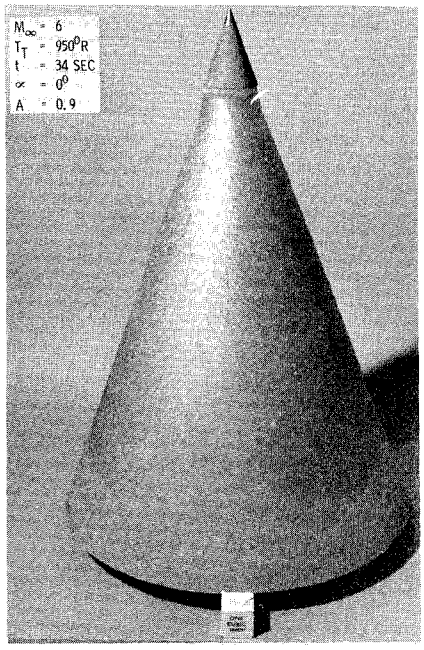

Fig. 4 20° camphor cone tested at surface pressure of 440 psf.

Results and Discussion

Camphor

Camphor was tested over a wide local cone surface pressure range (170–1110 psf). Either cross-hatching or a carved, regmaglypt ablation pattern was obtained over this entire pressure range as illustrated by Figs. 3–7. Pretest plans called for tests no lower than 400 psf; this was reduced as far as possible (to 170 psf) with the existing model geometry when cross-hatching was obtained at 400 psf. Cross-hatching appears in the post-test photographs only for the lower ablation ages (Figs. 3 and 4). Ablation age (A)[¶] is defined as the ratio of the thickness of material ablated away to the boundary-layer thickness at the same point:

$$A \equiv W/\delta$$

The boundary-layer thickness (δ) was estimated for the smooth-wall, nonablating conditions, except that boundary-layer transition was chosen to match the ablating case. All ablation age estimates shown herein are for the model trailing edge. Although Fig. 5 (at 640 psf) shows a carved, regmaglypt pattern, the film record of this test shows the surface was initially cross-hatched. Larson and Mateer reported similar results for camphor.[4] The two highest pressure tests, Figures 6 and 7, were conducted on opaque models which resulted from a poor vacuum during pressing. This is not believed to have had an appreciable effect on the resulting ablation pattern. Incidentally, the two holes in the left side of the 870 psf model (Fig. 6) are not imperfections, but are a result of special hole and protuberance tests. The black specks on the model shown in Fig. 4 are oil which struck after the model was retracted from the airstream. Figure 4–7 show the pointed steel tip and ceramic insulator design used on all models.

§ The manufacturer's designation of the low ablation temperature Korotherm referred to as "special Korotherm" is: 792–705 with 1% each of 910-781 and 914-700. Appreciative acknowledgement is made to G. W. Parker of DeSoto Inc., for suggesting and supplying the material.

¶ This parameter is believed to have been first suggested by C. du P. Donaldson.

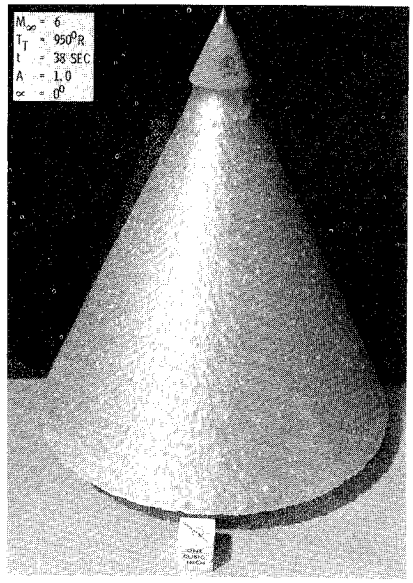

Fig. 5a 25° camphor cone tested at surface pressure of 870 psf.

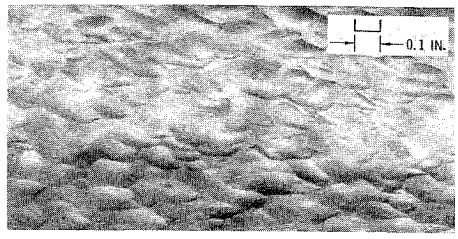

Fig. 5b Magnified view.

Some of the finer details of camphor ablation surface patterns can be seen in Fig. 3b (crosshatched), and Fig. 5b (regmaglypt). The variation of the streamwise length of the ablation patterns with the local surface pressure is shown in Fig. 8. The parametric use of pressure should not be taken to mean that it is the most fundamental or a key parameter in ablation pattern studies. A satisfactory theoretical explanation is still forthcoming and may well disclose better parameters. Meanwhile, pressure is a very useful variable and is fundamental in many other likely parameters such as

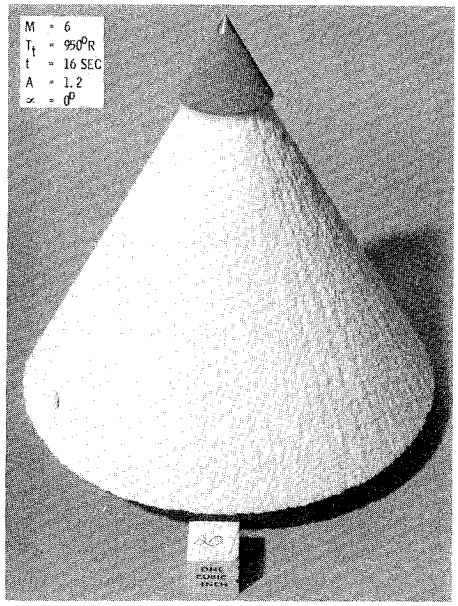

Fig. 6 30° camphor cone tested at surface pressure of 870 psf.

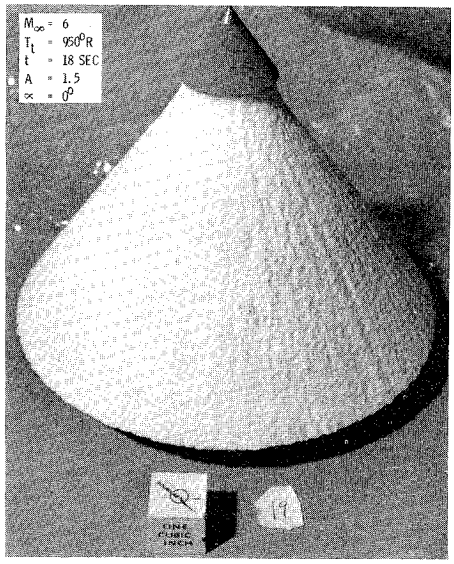

Fig. 7 35° camphor cone tested at surface pressure 1110 psf.

Reynold's number, boundary-layer thickness, ablation rate, ablation age, and so on.

Figure 3 shows the effect of shock impingement just ahead of the base of the lowest pressure model. The increased ablation rate in the higher pressure region aft of the shock intersection resulted in approximately 0.1 in. greater depth of ablation. Just ahead of shock impingement, cross-hatching was very faint, but the superimposed radial grooves were fairly distinct. The resulting surface for 1 in. aft of shock intersection was smooth, despite the considerably higher ablation; then a regmaglypt ablation pattern, characteristic of the higher pressure region behind the shock appeared. The epoxy cast (Fig. 9) shows this better than the model itself. (Unfortunately, the thin rubber mold deflected when the cast was made resulting in the round depression and other imperfections just ahead of shock impingement.) It is notable that there were only streamwise grooves and cross-hatching—no regmaglypt pattern—ahead of the shock and that there were no radial grooves aft of the shock.

Naphthalene

Naphthalene was tested primarily to determine the effect of a liquid layer on ablation patterns. Naphthalene is similar in many respects to camphor. Their phase diagrams, Fig. 10, are similar, except that the triple point of naphthalene is at a much lower pressure than that of camphor. For the test conditions indicated in this figure, camphor sublimes, but naphthalene has a liquid layer plus vaporization and this was borne out by experiment. A liquid layer flowing off the

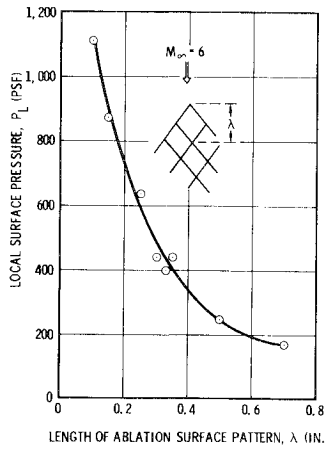

Fig. 8 Variation of camphor ablation surface pattern length with local surface pressure.

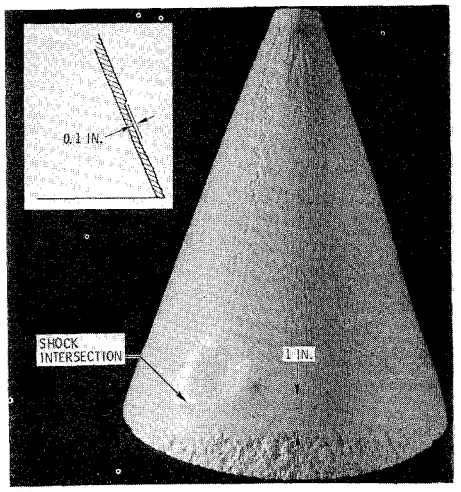

Fig. 9 Shock impingement—epoxy cast of camphor model of Fig. 3.

rear of the naphthalene model was recorded by the test film and post-test observation showed a glossy surface that resulted from the freezing of the liquid layer when the model was removed from the tunnel stream. The ablation surface patterns appear similar, although the naphthalene pattern is coarser. Figures 6 and 11 show the 30° camphor and naphthalene models tested under the same conditions. The irregular trailing edge of the post-test naphthalene model was formed by the freezing of the liquid layer. The cavity shown by the photograph resulted from a model imperfection.

Radial Grooves

Radial grooves, characteristic of the laminar flow believed to exist near the vertex, are shown in Figs. 3–6. Radial grooves can also be seen superimposed on the crosshatched or regmaglypt patterns over the remainder of the conical models for the lowest pressure (Fig. 3) and the highest pressures (Figs. 6 and 7). All camphor models developed such grooves, but in some cases they are too weak to be seen in the photograph. Larson and Mateer reported similar results for camphor.[4,6] Streamwise grooving in the presence of a liquid layer is shown in Fig. 11 for the naphthalene model. Radial grooves were wiped out by shock impingement. Radial grooves are believed related to Görtler vortices.[15] In an attempt to encourage radial grooves, a concave camphor

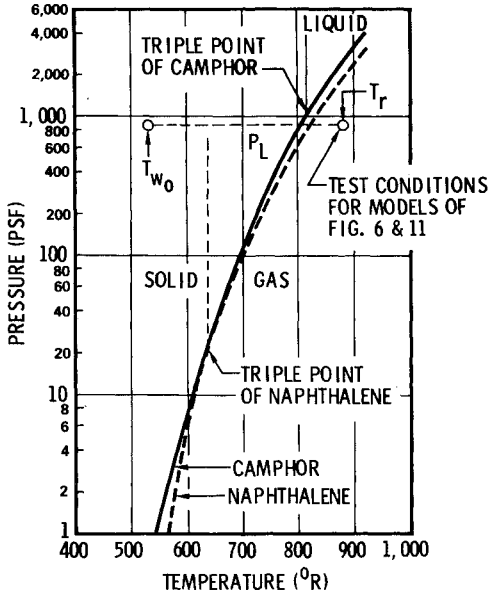

Fig. 10 Phase diagrams for naphthalene and camphor.

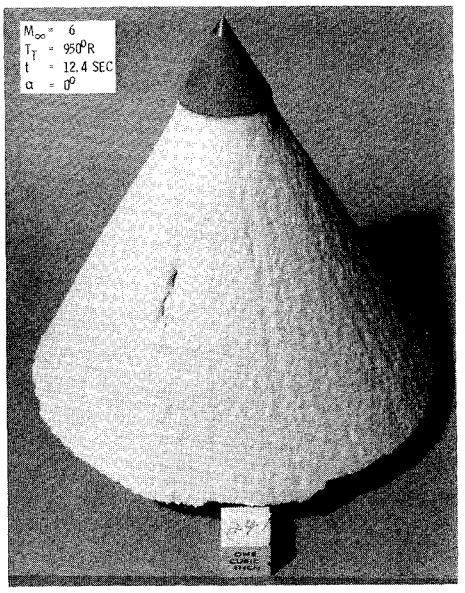

Fig. 11 30° naphthalene cone tested at surface pressure of 870 psf.

model was tested. The resultant ablation surface patterns were similar to those of conical models of equivalent local surface pressure. No extension of the region of only radial grooves near the vertex was noted and the remainder of the ablated surface consisted of regmaglypt patterns with radial grooves superimposed. Of course, the curvature machined into this model was much less than that created by ablation immediately aft of the nose tip. Larson and Mateer noted the effect of steel tips.[4] Tobak suggested vortices as the origin of cross-hatching.[16]

During the planning of these tests, because of the presumed phenomenology requirement for either transitional or turbulent flow, it was suggested that ablation in the presence of boundary layer transition might be essential to the formation of ablation-surface patterns; consequently, a partial camphor ablation model (Fig. 12) was tested at the same wind-tunnel conditions as the model of Fig. 6. Boundary-layer transition occurred on the nonablating aluminum surface as planned. The ablated surface appeared almost identical to that of Fig. 6, except that the radial grooves superimposed on the regmaglypt pattern were barely perceptible.

Special Korotherm

Figure 13 shows a cross-hatched pattern ablated in special Korotherm in the wind tunnel. It appears remarkably similar to the pattern of a recovered hypervelocity vehicle that had a charring ablator of phenolic, fused-silica-fiber composite. (See Ref. 4 Fig. 4b or Ref. 9 Fig. 1b). Since special Korotherm was a new and experimental material, fewer test runs were planned for it than for camphor, and some runs did not develop the anticipated patterns. The

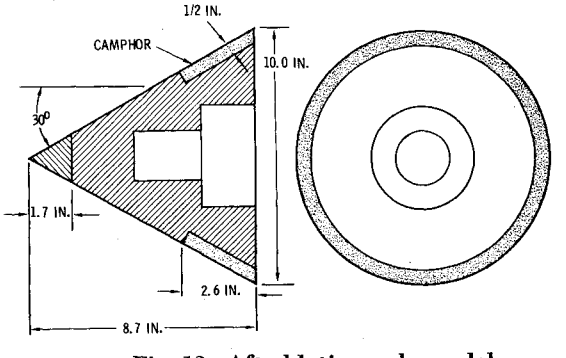

Fig. 12 Aft ablation only model.

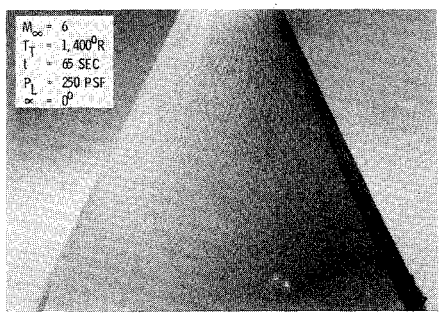

Fig. 13 25° special korotherm cone.

first special Korotherm models were made by troweling the material on the aluminum core. Later models were cast. The troweled-on material ablated as a liquid, and cast models sublimed. Liquid ablation started sooner, but showed a similar cross-hatched pattern which was wiped out by surface tension and solidification of the liquid at the end of the run. Measurements of the liquid pattern angles from the film show them to be approximately the same as for the subliming pattern angles for the same test conditions. One test was performed with liquid ablation side by side with sublimation on the same model. The post-test frozen liquid is shown at

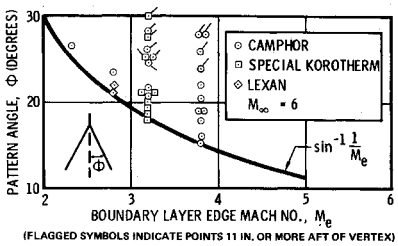

Fig. 14 Surface pattern angle as a function of local Mach number-MDAC West Test.

the far right of Fig. 13. The difference in ablation mode arises from the fact that the Korotherm resin mechanisms are air inhibited. The cast models cured thoroughly, whereas the trowled model surface, being exposed to air, did not.

Pattern Angle

Figure 14 shows the pattern angles obtained in the tests. The flagged symbols indicate data obtained 11 in. or more (slant length) aft of the vertex, and the plain symbols indicate

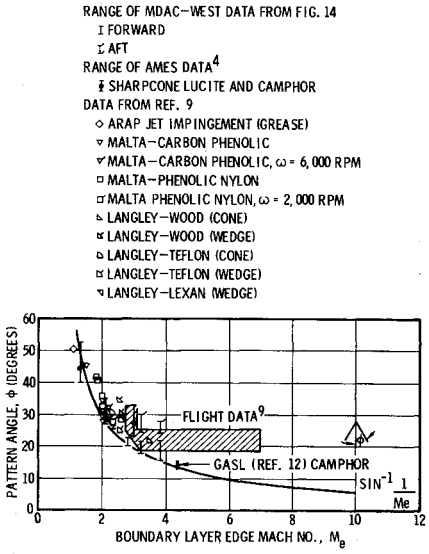

Fig. 15 Surface pattern angle as a function of local Mach number.

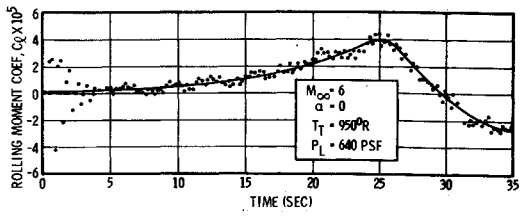

Fig. 16 Roll torque of ablating camphor 25° cone.

pattern angles within 9 in. of the vertex. Despite considerable scatter, appreciable increase in the aft pattern angles is obvious. This was also obvious from examination of the longer models. The pattern angle correlation with boundary-layer-edge Mach number noted in Refs. 4, 8, and 9 is confirmed by these data except there is no indication of a limiting minimum angle above Mach 3 as suggested by the flight data.[7] Also, the maximum scatter band of about 13° is the same. This scatter can be halved, at least for the present tests, by considering only points from the forward part of the models. A collection of data from Refs. 4 and 9, and one point from Ref. 12, is shown in Fig. 15 together with the MDAC-West data. Reference 8 gives an additional 60 points at boundary-layer edge Mach numbers 1 to 3. These data are compatible with those of Fig. 15.

Roll Torques

Variation of roll torque with time for an ablating camphor cone is shown in Fig. 16. This model is the same as that shown in Fig. 5. The rolling moment coefficient is referenced to the model base diameter and area. The scatter during the first few seconds results from a small amplitude roll oscillation of the model at its natural roll frequency of about 3 cps when the model was inserted into the tunnel stream. The film records show that cross-hatching developing on an oscillating model is fixed on the model and rotates with it.** Laganelli and Nestler show that constant spin rates of 2000 to 6000 rpm merely result in a skewing of the ablation pattern by the resultant effective flow angles.[9]

Figure 17 shows the roll torque measurements for a Lexan cone. The model was tested first at a total temperature of 950°R, and it did not ablate. The same model was then polished to remove any roughness that resulted from the previous test and tested again at a temperature of 1120°R where it did ablate, leaving a surface pattern characteristic of Lexan. As the figure shows, the model had an initial roll torque coefficient of about 2×10^{-5} due to aerodyanmic asymmetry. As anticipated, the initial roll moment coefficient remained essentially constant on the nonablating model and was approximately repeated when the model was again mounted in the wind tunnel and rerun.

Price and Ericsson have demonstrated that a small normal force can produce appreciable roll torque.[17] Although not quantified, the pointed nonablative nose tips used on the

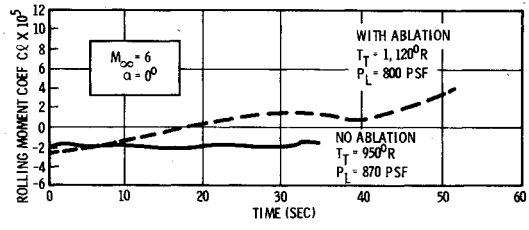

Fig. 17 Roll torques of 30° lexan cone.

** The film records also show that particle impingement (debris from the pebble-bed heater common to most hypersonic wind tunnels) did not appear to affect the ablation surface patterns. The tiny craters that resulted from particle impact faded away with ablation without changing the patterns.

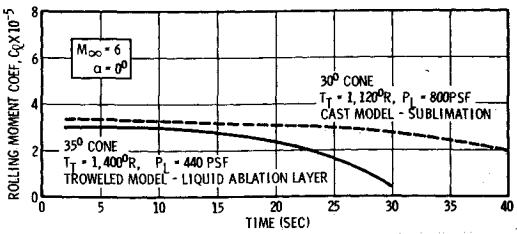

Fig. 18 Roll torques of ablating special korotherm cones.

models of the tests reported here limited variation of normal force asymmetry by ablation, particularly at zero angle of attack. Consequently, the variation in rolling moment coefficient with time for the ablating model is believed to be caused primarily by the ablation surface pattern.

Roll torques of two special Korotherm models are shown in Fig. 18. The 30° cone was a cast model, and it sublimed (Fig. 20 of Ref. 11). The 35° cone was a troweled model, which ablated in a melting mode.

The previous data were all taken at a zero angle of attack. The few angle-of-attack runs show appreciably greater variation of roll torque, as indicated by Fig. 19 for a 30° camphor cone at an angle of attack of 5°. More data are needed to confirm this. At least part of this increased torque variation is probably due to ablation-induced normal force asymmetry which is more likely and more potent at angle of attack. Unfortunately, it is impossible to make a quantitative torque source breakdown with only rolling moment measurements. There were no surprises in the ablation surface patterns at angle of attack; the patterns follow the streamlines, and the local size and pattern angle reflects the local pressure.

Conclusions

An experimental investigation of ablation surface patterns and resulting roll torques on pointed, conical models has been conducted in a Mach 6 wind tunnel with a variety of low-temperature ablators. Because the subject of surface ablation patterns is relatively new and this is the first report of direct measurements of roll torque during the ablation process, the following conclusions are tentative and subject to modification as more data and a better understanding of the phenomenon develops.

1) Either cross-hatching or a regmaglypt pattern was obtained on camphor for the entire range of local surface pressure tested (170–1110 psf).

2) The scale of cross-hatching decreases with increasing pressure for camphor.

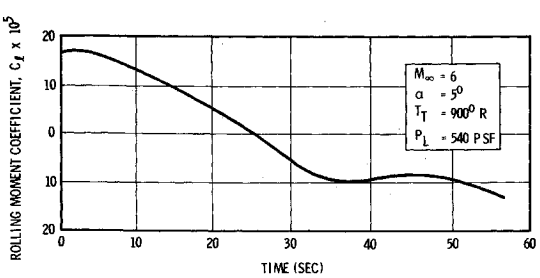

Fig. 19 Roll torque of 30° camphor cone at angle of attack.

3) The pattern angle trend with local Mach is similar to that of previous wind-tunnel tests.

4) The ablation pattern of melting-vaporizing naphthalene is similar to that of subliming camphor.

5) Wind-tunnel cross-hatching of subliming Korotherm is similar to that of silica phenolic from flight.

6) Roll torque variation appears to increase with angle of attack.

References

[1] Feldmann, S., "On the Instability Theory of the Soft Melted Surface on an Ablating Body when Entering the Atmosphere," Research Rept. 34, Aug. 1958, Avco Research Lab., Everett, Mass.

[2] Chapman, D. R., Larson, H. K., and Anderson, L. A., "Aerodynamic Evidence Pertaining to the Entry of Tektites into the Earth's Atmosphere," TR R-134, 1962, NASA.

[3] Chapman, D. R. and Larson, H. K., "The Lunar Origin of Tektites," TN D-1556, Feb. 1963, NASA.

[4] Larson, H. K., and Mateer, G. G., "Cross-Hatching—A Coupling of Gas Dynamics with the Ablation Process," AIAA Paper 68-670, Los Angeles, Calif., 1968.

[5] Canning, T. N., Wilkins, M. E., and Tauber, M. E., "Boundary-Layer Phenomena Observed on the Ablated Surface of Cones Recovered after Flights at Speeds up to 7 Km/Sec," CP-19, Vol. 2, 1967, AGARD.

[6] Larson, H. K. and Mateer, G. G., "Transition Measurement on Cones in Hypersonic Flow and Preliminary Observations on Surface Ablation Grooves," Rept. BSD TR 67-213, Vol. III, Sec. 17, Aug. 1967, U.S. Air Force.

[7] Canning, T. N., Wilkins, M. E., and Tauber, M. E., "Ablation Patterns on Cones having Laminar and Turbulent Flows," *AIAA Journal*, Vol. 6, No. 1, Jan. 1968, pp. 174–175.

[8] Canning, T. N., Tauber, M. E., Wilkins, M. E., and Chapman, G. T., "Orderly Three-Dimensional Processes in Turbulent Boundary Layers on Ablating Bodies," CP-30, 1968, AGARD.

[9] Laganelli, A. L. and Nestler, D. E., "Surface Ablation Patterns: A Phenomonology Study," *AIAA Journal*, Vol. 7, No. 7, July 1969, pp. 1319–1325.

[10] Claar, H. O., "The Douglas Aerophysics Laboratory Two-Foot Hypersonic Wind Tunnel," DAC Rept. 59808, Oct. 1967, McDonnell Douglas Astronautics Co.—West, El Segundo, Calif.

[11] Williams, E. P., "Experimental Studies of Ablation Surface Patterns and Resulting Roll Torques," AIAA Paper 69-180, New York, 1969.

[12] Lipfert, F. W. and Genovese, J., "An Experimental Study of the Boundary Layer on Low Temperature Subliming Ablators," TR 688, Feb. 6, 1968, General Applied Science Labs., Westbury, N.Y.

[13] Sayano, S., "Investigation of the use of Low-Temperature Materials for Studies of Ablation and Sublimation in Supersonic Flow," Master's thesis, Oct. 1962, Univ. of California, Los Angeles.

[14] Charwat, A. F., "Exploratory Studies on the Sublimation of Slender Camphor and Naphthalene Models in a Supersonic Wind-Tunnel," RM-5506-ARPA, July 1968, The Rand Corp., Santa Monica, Calif.

[15] Görtler, H., "On the Three-Dimensional Instability of Laminar Boundary Layers on Concave Walls," TM 1375, 1954, NACA.

[16] Tobak, M., "Hypothesis for the Origin of Cross-Hatching," *AIAA Journal*, Vol. 8, No. 2, Feb. 1970, pp. 330–334.

[17] Price, D. A., Jr. and Ericsson, L. E., "A New Treatment of Roll-Pitch Coupling for Ballistic Re-Entry Vehicles," *AIAA Journal*, Vol. 8, No. 9, Sept. 1970, pp. 1608–1615.